Environmental Science and Pollution Research (2023) 30:6201–6215
https://doi.org/10.1007/s11356-022-22619-3

RESEARCH ARTICLE

Fenton oxidation catalysed by heterogeneous iron–perlite for 8-hydroxyquinoline-5-sulfonic acid (8-HQS) degradation: efficiency comparison using raw and calcined perlite as precursors for iron fixation

Ibtissem Boumnijel[1] · Najwa Hamdi[2] · Houda Hachem[1] · Hedi Ben Amor[3] · Daoued Mihoubi[1]

Received: 26 May 2022 / Accepted: 16 August 2022 / Published online: 22 August 2022

Abstract
Herein, the catalytic activity of two types of iron-loaded perlite catalysts prepared by impregnation of raw and calcined perlite in terms of 8-hydroxyquinoline-5-sulfonic acid (8-HQS) degradation was investigated by the Fenton reaction. Different iron contents were used to optimize the Fenton catalytic reaction. The as-prepared catalysts were characterized using different spectrophotometry techniques. The effect of some operating parameters on the Fenton oxidation of 8-HQS was carried out. Iron content of 10% has led to the highest catalytic efficiency. Furthermore, the oxidation of 8-HQS is highly affected by the addition of H_2O_2, proposing that the heterogeneous Fenton reaction has been successfully activated. Whatever the type of the used catalyst, the heterogeneous catalytic oxidation process is extremely rapid, even instantaneous. The synthesized catalysts remained potentially active and retained their catalytic activity for successive Fenton reactions suggesting their economic benefit over the homogenous Fenton process. Accordingly, the newly prepared heterogeneous solid could be successfully used to treat wastewater effluents containing persistent organic compounds.

Keywords Heterogeneous catalyst · Fenton process · 8-hydroxyquinoline-5-sulfonic acid · Perlite · Calcined perlite

Introduction

During manufacturing processes, wastewater effluents containing persistent organic compounds, extremely harmful to humans and the environment, are discharged into the natural surroundings. Facing the fast developments of the industrial sector activity, many environmental problems have submerged, and therefore, more efforts are required to rescue the planet. To overcome water pollution by aromatic compounds, the development of cost-effective and environmentally friendly technologies is highly commended by both the scientific and industrial communities. Conventional techniques based on physical, chemical, and biological methods, such as coagulation, adsorption, ion exchange, and ultrafiltration, are inefficient to remove persistent organic compounds in wastewater considering their persistence in the environment, resistance to microbial attack, and temperature as well as ability to bio-accumulate in ecosystems. Advanced oxidation process (AOP) is an advanced treatment process that involves the generation of non-selective and highly hydroxyl-free radicals (·OH) readily capable of degrading numerous organic, toxic, and biologically resistant compounds in wastewater by converting them to less harmful intermediate products (Buthiyappan et al. 2016; Grčić et al. 2010; Tekin et al. 2006). As an advanced oxidation process, Fenton process is widely used to treat wastewaters contaminated with persistent organic compounds. Compared to the other conventional AOPs, Fenton reaction is a cost-effective and efficient process owing to the large production

Responsible Editor: Ricardo A. Torres-Palma

✉ Ibtissem Boumnijel
ibtissem.boumnijel@hotmail.fr

[1] Laboratory of Wind Energy Management and Waste Energy Recovery, Research and Technology Center of Energy, B.P. 95, Hammam-Lif 2050, Tunisia

[2] Research Unit of Electrochemistry, Materials and Environment (RU:EME), Faculty of Sciences of Gabes, University of Gabes, St Erriadh, 6027 Gabes, Tunisia

[3] Research Laboratory of Processes, Energetic, Environment and Electric Systems (PEESE), National School of Engineers of Gabes (ENIG), 6072 Gabes, Tunisia

of highly reactive radicals ·OH, fast mass transfer, short treatment, simplicity and low cost (Babuponnusami and Muthukumar 2014, Bautista et al. 2008, Wang et al. 2016, Zhang et al. 2019). Some of the major drawbacks of the homogenous Fenton process are sludge formation, deactivation of catalyst by some iron complexing agents, the cost of reagent consumption, difficulty in catalyst recycle and reuse, pH dependence and high energy consumption (Wang et al. 2016; Xu et al. 2020; Zhang et al. 2019). To address these limitations, most of the research community are currently trying to convert the Fenton process into a heterogeneous process by prepared solid oxides and composites such as modified MOFs (Dapaah et al. 2022; Du et al. 2022; Joseph et al. 2021; Wang et al. 2022), ferrite nanoparticles (Soufi et al. 2021), metal nanoparticles and iron fixed on biochar (Deng et al. 2018), on activated carbon (ACs) (Briton et al. 2019; Fontecha-Cámara et al. 2011; Navalon et al. 2011; Ramirez et al. 2007), and on clays and zeolites (Hartmann et al. 2010; Navalon et al. 2010; Poza-Nogueiras et al. 2018) and so forth.

When compared to homogeneous Fenton, heterogeneous Fenton has several advantages and disadvantages. (i) As advantages, heterogeneous Fenton can combine adsorption and catalytic Fenton reaction in the same reaction medium (Baloyi et al. 2018). (ii) Heterogeneous catalysts are recoverable and reusable. (iii) High amount of by-products can be adsorbed on the surface of the heterogeneous catalyst resulting in low by-product formation. (iv) Heterogeneous Fenton can overcome the restricted pH range generally adopted in homogeneous Fenton oxidation systems without the formation of iron-based sludge (Soufi et al. 2021; Zhang et al. 2019). In terms of disadvantages, (i) the catalytic Fenton reaction is mainly performed on the catalyst surface, whereas in the homogenous Fenton process, the oxidation takes place in the reaction medium without any mass transfer limitations. (ii) When compared to homogeneous Fenton reactions, heterogeneous Fenton produces a lower yield of ·OH and, in some situations, require a greater dose of H_2O_2.

Nevertheless, extensive research is required to explore the efficiency of many natural and abundant materials as precursors or supports. In this regard, the use of a siliceous rock like perlite as a natural material with a mineral structure seems to be interesting. Perlite, an amorphous volcanic glass, is an abundant, cheap, chemically inert and environment-friendly media (Khudr et al. 2021). It is widely used in industries (dyeing, food, drug, fuel oil, filter aid, filler in paint, enamels, glazes, plastics and resins, etc.) and construction (Jahanshahi and Akhlaghinia 2015). Calcined perlite, resulted usually from a thermal treatment, has several advantages, including light weight, high porosity along with strong adsorbability, thermal and chemical stability, mechanical resistance, low cost, low toxicity, non-corrosiveness and ease of handling (Jahanshahi and Akhlaghinia 2015, Kolvari et al. 2015). The extremely high porous structure of raw and calcined perlite, the amorphous silica content (Si–O–Si) and the high number of surface hydroxyl groups (Si–OH) that enhance metal immobilization (Buthiyappan et al. 2016; Khudr et al. 2021; Kolvari et al. 2015; Maryami et al. 2017) make them excellent supports for the preparation of heterogeneous catalysts. Moreover, the loosely bound nature of perlite allows the exchange of other types of metals, especially iron, in an aqueous solution. Accordingly, by having the ability to fix iron ions as catalytic active sites on its surface, iron-coated perlite exhibits both high adsorptive capacity and catalytic activity under a stable physical state. It is to highlight that several iron-coated perlite catalysts were reported as photo-Fenton catalysts (Jiang et al. 2017; Puga et al. 2020), but they have not been profusely explored as heterogeneous Fenton ones.

This research aims to fabricate iron-coated perlite as a heterogeneous Fenton catalyst for the oxidation of organic pollutants in water, i.e. 8-HQS as a model molecule. Given that the nature and structural properties of support play a crucial role in modulating the Fenton oxidation reaction in the catalytic sites, two types of supports were used, mainly raw and calcined perlite. The heterogeneous catalysts were fabricated by impregnating iron sulphate (II) onto perlite. For comparison purposes, the catalytic activity of the as-prepared catalysts was investigated. The influence of all key factors (initial pH, reaction time, catalyst dosage, molar oxidation ratio H_2O_2/8-HQS, temperature and initial concentrations of 8-HQS) that contribute to the enhancement of the degradation efficiency of 8-HQS in aqueous solution was carefully explored and evaluated. The reactivity, reusability and stability of the catalysts during reactions were reported.

Materials and methods

Materials

Perlite samples which contained 77.16% SiO_2 and 14.68% Al_2O_3 were provided from EUROPERLITA. The 8-HQS with 99% purity was purchased from SIGMA Aldrich. Hydrogen peroxide (H_2O_2) (30%, w/w) is a commercial solution (30%) purchased from PARACHIMIC (Sfax). Determined before each trial, its concentration was performed by the iodometric method.

Iron sulphate (II) ($FeSO_4{\cdot}7H_2O$) was of analytical grade. It was used to prepare the iron-coated perlite and had been supplied by LABOSI (French). Sulphuric acid (H_2SO_4), sodium thiosulfate ($Na_2S_2O_3$), potassium iodide (KI) and sodium hydroxide (NaOH), all in analytical grade, were obtained from PROLAB (Tunisia), LABOSI (French)

and SIGMA ALDRICH (USA) and used without further purification.

Characterization

The catalyst crystallinity was analysed by powder X-ray diffraction (XRD) on a D8 Advance diffractometer (Bruker, Germany). The range of scanning angle (2θ) was kept at 5–80°. Fourier transform infrared spectroscopy (FTIR) was recorded using a Bruker VERTEX 80v vacuum FT-IR spectrometer at the wavenumbers of 400–4000 cm^{-1}. The thermal stability of the prepared catalysts was resolved by thermal gravimetric and differential thermal analysis (TGA-DTA) measurements from 50 to 1000 °C by the heating rate of 10 °C min^{-1} using a TGA/DSC 3 + METTLER TOLEDO Instrument.

Microscopic image observation of raw perlite, calcined perlite and the prepared catalysts was performed using two digital processing units composed of a conventional optical microscope, a camera and a PC/Notebook irrespective of the used microscope. The first optical microscope of the type Zeiss Stemi 2000-C Stereo (zoom range: 6.5 × –50 ×) has been used to illustrate sample images. The second optical microscope of type Axioskop 40 (zoom range: 200 × /0.45, Infinity/0.17) is equipped with several magnifications: correction, filtering, and a potentiometer to adjust the light level and have the proper contrast. Depending on the image's nature, two microscopy and contrasting techniques are used with the Axioskop 40 microscope, namely transmitted and reflected lights. The microscope camera is a Power Shot G9 type, and it is separately connected to the microscope camera via a video capture card (Remote Capture DC). For the image observations, the powder samples have been directly dispersed on a microscope slide.

Preparation of iron-loaded perlite

Raw perlite was washed with distilled water several times to remove impurities, mainly dust. The collected material was stirred for 6 h in 100 ml ethanol and peroxide hydrogen (30%) to remove organic components, rinsed with excess deionized water and then dried at 105 °C for 24 h to remove the moisture content. The calcination process of raw perlite was performed at 1050 °C as reported by Boddu et al. (2009).

Two types of catalysts were prepared by the impregnation of raw and calcined perlite (RP and CP) (2 g) with an iron sulphate solution ($FeSO_4 \cdot 7H_2O$) (200 ml) according to the following mass ratios: 1%, 5% and 10% (m(Fe)/m(perlite)). Each dispersion was stirred for 2 h in a closed 250-ml Glass Flask Erlenmeyer at 300 rpm to adsorb the iron ions on the surface of the corresponding support. The dispersions were then dried in an oven for 1 h at 105 °C before being subjected to an additional heat treatment in a drying oven for 3 h at 280 °C. It should be noted that the name of the synthesized catalyst is given by *NP-x*% Fe of which '*N*' designates the nature of the perlite '*R*: raw or *C*: calcined', and '*x*' presents the increasing iron impregnation ratio: 1%, 5% and 10%.

Fenton experiments

Batch experiments of the catalytic oxidation of 8-HQS were conducted in a closed 250-ml Glass Erlenmeyer Flask at different temperatures ranging from 25 to 90 °C to investigate the effect of different controlling parameters, such as initial pH, reaction time, initial concentration of 8-HQS, oxidation ratio and catalyst dosage. Samples of 100 ml at varying initial concentrations of 8-HQS ranging from 0.1 to 0.4 mM were heated to the desired temperature after adjusting their initial pH value to an optimized value using 1 M NaOH solution. A predetermined amount of the tested catalyst (5–25 mg) was introduced to the reaction medium and vigorously stirred to ensure its dispersion. Afterward, H_2O_2 was added for the Fenton oxidation at different molar ratios of H_2O_2: 8-HQS ranging from 5 to 40. Aliquots of the reaction medium were sampled periodically, filtered using a 0.22-µm porosity syringe filter and then analysed with a UV–Visible spectrophotometer.

The removal efficiency of 8-HQS, evaluated as the rate of discoloration of the treated solution, was calculated using Eq. 1. The residual concentration of 8-HQS was determined by measuring the absorption intensity of the reaction medium sample at a wavelength of 306 nm using a UV–Visible spectrophotometer of type C-7100 PEAK Instruments. To reduce measurement errors, the UV absorption intensity of each sample was measured in triplicates. The average value makes it possible to calculate the residual concentration of 8-HQS:

$$\text{Removal rate } (\%) = \frac{C_0 - C}{C_0} \times 100 \quad (1)$$

where C_0 and C are the concentrations of 8-HQS initially and at a given time t, respectively.

Results and discussion

Characterization of catalysts

XRD analysis

X-ray diffraction (XRD) technique was used to investigate structural changes that could have occurred in raw and calcined perlite after iron fixation. Accordingly, the crystallinity

of the synthesized catalysts RP-10% Fe and CP-10%Fe was analysed using the XRD patterns presented in Fig. 1.

The XRD pattern of raw perlite did not display clear and sharp diffraction peaks, as illustrated in Fig. 1, showing that perlite is mostly amorphous in nature (Jiang et al. 2017). RP is mainly composed of amorphous mineral phases noticed between 15° and 30° which are in good agreement with the literature review (Ahmed et al. 2020; Saufi et al. 2020). After calcination, the amorphous structure of CP has not been practically modified except for the intense peak at 43.19°. By comparing the pattern of RP-10% Fe and CP-10%Fe with RP and CP respectively, the patterns of the synthesized catalysts exhibit eight diffraction peaks from 27.93° to 78° (2Θ) and a new amorphous dump between 38° and 45° possibly ascribed to $FeSO_4$. The sharp diffraction peak associated to the new amorphous dump in the CP-10%Fe pattern points out its high structure order degree and crystallinity, which seems obvious after the calcination step. Whatever the used support, the amorphous dump characterizing the amorphous structure of perlite has shifted to higher angles from 25° to 37° (2θ) after iron incorporation. This shifting confirms the efficient incorporation of iron into the crystal surface of the synthesized catalysts.

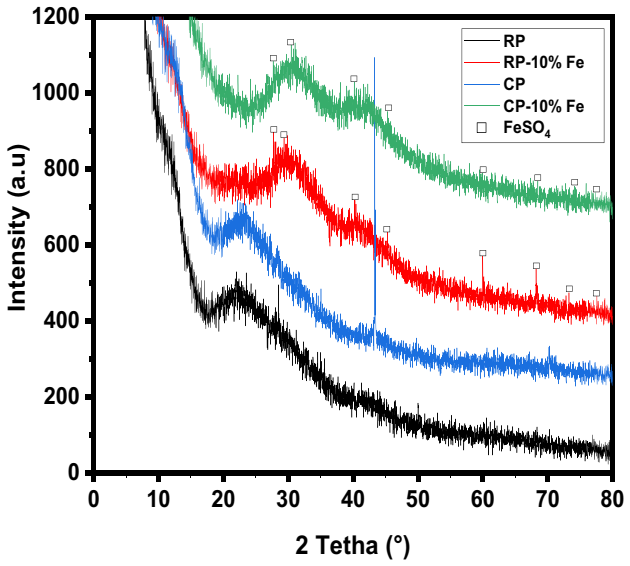

Fig. 1 XRD patterns of the RP, CP and the synthesized catalysts (RP-10% Fe and CP-10%Fe)

FTIR

To assess the effective fixation of iron on perlite through the detection of chemical bonds on its surface, FT–IR spectra of RP, CP and the as-prepared catalysts were recorded and are displayed in Fig. 2.

According to the IR spectrum of RP, it is clear that there are five significant absorption bands as identified in the literature review (Ahmed et al. 2020; Brindha et al. 2019; Esmaielpour et al. 2017; Puga et al. 2020). The indicative

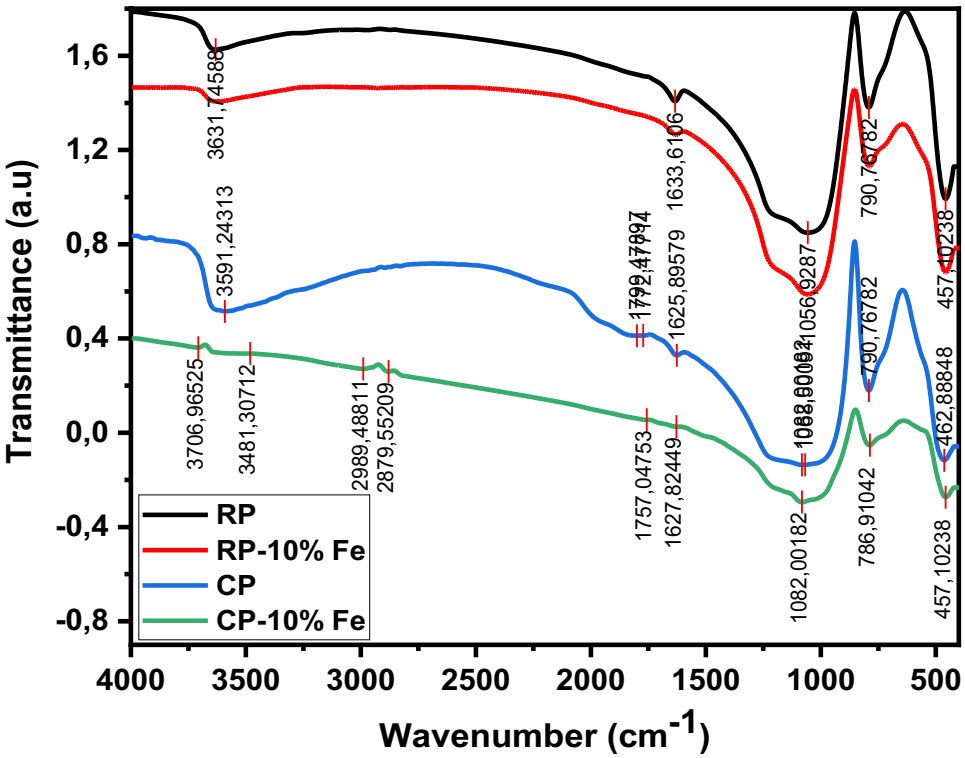

Fig. 2 FTIR spectrum of RP, CP and the synthesized catalysts (RP-10% Fe and CP-10%Fe)

bands attributed to the stretching and bending vibrations of hydroxyl groups (OH) on the perlite surface (mainly free Si–OH groups) and the adsorbed water molecules are shown at 3631.75 cm^{-1} and 1633.61 cm^{-1}, respectively (Kolvari et al. 2015; Puga et al. 2020; Saufi et al. 2020). The large band centred at 1056.93 cm^{-1} and the peak located at 790.77 cm^{-1} are assigned to the Si–O stretching vibrations of Si–O–Si and Si–O–Al, respectively (Papa et al. 2018; Saufi et al. 2020). At about 457.10 cm^{-1}, O–Si–O bending vibrations are obvious (Esmaielpour et al. 2017). The FTIR spectrum of RP and RP-10% Fe are quite similar. Nevertheless, RP-10% Fe showed as compared to RP a higher intensity peak at 1056.93 cm^{-1} and a slight broadening of the absorption band at 3631.75 cm^{-1} which clearly indicates the incorporation of iron on its surface.

The FTIR spectrum of CP-10% Fe is significantly deformed when compared to RP, CP and RP-10% Fe. In comparison to the CP, bands located at 400–4000 cm^{-1} were sharply decreased in the CP-10% Fe sample wherein the SiO–H stretching vibrations at 3591.24 cm^{-1} were barely observed suggesting the successful fixation of iron ions. In addition, new small bands are observed at 3706.97, 2989.77, 2879.49 and 2879.55 cm^{-1}. It is worthy to note that iron is adsorbed on the solid porous surface of perlite thanks to both the physisorption generated by Van der Waal's forces and chemisorption caused by valence forces through the spontaneous formation of chemical bonds especially with Si–OH groups and Si–O stretching vibrations (Khudr et al. 2021). According to the foregoing discussion, the above-mentioned modifications demonstrate that iron particles are definitely loaded and firmly immobilized on the surface of raw and calcined perlite.

TGA-DTG of the catalysts

The thermal stability of RP, CP and the synthesized catalysts was studied using Thermal gravimetric and differential thermal analysis (TGA-DTG). TGA thermogram of RP, presented in Fig. 3a, shows two endothermic peaks, as is typical in the literature. The significant initial weight loss of 14.77% occurs at 166.19 °C whereas a second weight loss of 5.65% happens at 213.65 °C. The heat treatment in the range 150 to 200 °C serves mainly to vaporize water without driving it out of the sample (Bagdassarov et al. 1999, Esmaielpour et al. 2017, Roulia et al. 2006); therefore, the first peak is defined as the temperature of glass dehydration while the second peak corresponds to the main water release from the amorphous structure of the perlite (Bagdassarov et al. 1999). After that, a steady weight loss up to 980 °C is likely attributed to the gradual dehydroxylation of perlite.

The TGA of RP-10% Fe (Fig. 3b) shows two mass losses below 250 °C ascribed to the elimination of perlitic water molecules, then a third one at 507.48 °C that can be attributed to iron mass loss. Nevertheless, the DTG curve of CP-10% Fe (Fig. 3c) has only one peak at 599.33 °C. There are no additional peaks related to the elimination of perlitic water given that the trapped water has been already vaporized during the calcination step. Accordingly, this latter peak can only be attributed to iron loss. It is worth noting that the iron mass loss in RP-10% Fe is substantially more than in CP-10% Fe, suggesting that RP is more incorporated with iron ions.

Morphology analysis

Using the digital processing units related to the two optical microscopes, selected images for the RP, CP, RP-10%Fe and CP-10%Fe were employed to show the surface morphological changes occurring on the catalysts due to the incorporation of iron on the surface of raw and calcined perlite. The glassy and amorphous nature of perlite is clearly evident in the optical images (Fig. 4a and b). In view of the aforementioned characteristics of perlite, the calcination step has promoted the formation of regular and larger crystals as well as regular clusters in three dimensions (Fig. 4b). The examination of the images illustrated in Fig. 4 reveals that the surface morphology of the raw and calcined perlite appears to change significantly following coating with iron ions. As shown in Fig. 4b and c, red dots and outlines on and around the perlite crystals confirmed successfully deposited iron species on the raw perlite structure.

Preliminary study of the Fenton catalytic oxidation of 8-HQS

Given that it is responsible for the activation of H_2O_2, the iron content incorporated on the surface of the perlite plays a crucial role during the catalytic oxidation of 8-HQS. Hence, three types of catalysts were tested: CP-1%Fe, CP-5%Fe and CP-10%Fe. Meanwhile, the effect of the reaction time was also investigated.

As shown in Fig. 5a, the catalytic oxidation reaction using CP-10%Fe coupled with H_2O_2 is instantaneous. A reduction rate of 46.72% is reached after the first minute, and then it is slightly increased to be eventually stabilized up to a reaction time of 2 h. Since the removal rate of 8-HQS is almost constant for the first 30 min, the catalytic activity of the catalyst will be only assessed during this period. Moreover, the higher the iron contents on the catalyst surface, the higher the degradation rate of 8-HQS (Fig. 5b). In fact, after 30 min, removal rates of 39.45, 65.75 and 82.43% are reached, with iron contents of 1, 5 and 10%, respectively. This improvement is expected since more active sites are available, resulting in higher production of hydroxyl radicals. To further assess

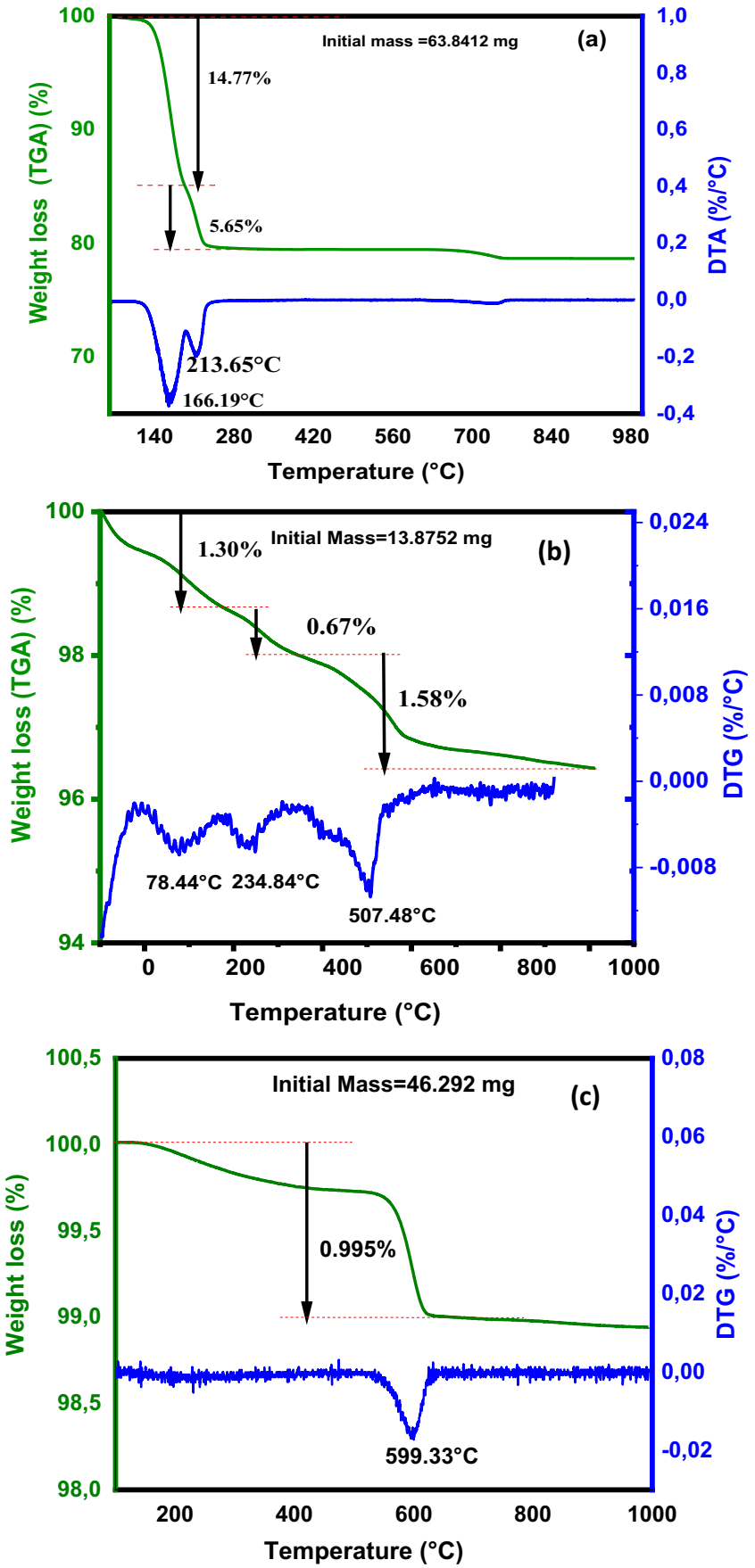

Fig. 3 TGA-DTA of **a** RP, **b** RP-10%Fe and **c** CP-10%Fe

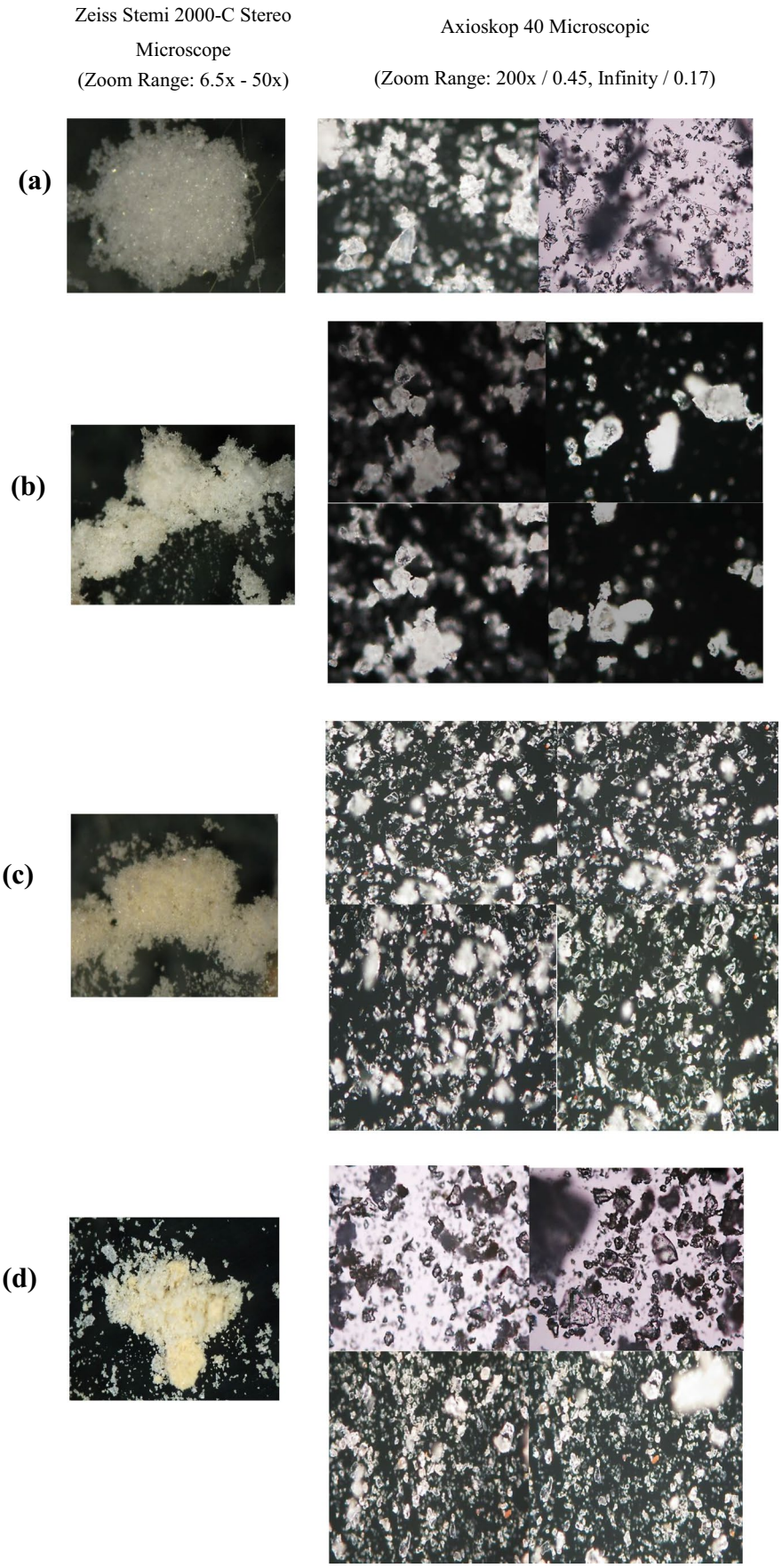

Fig. 4 Microscopic images of **a** raw perlite, **b** calcined perlite, **c** RP-10%Fe and **d** CP-10%Fe

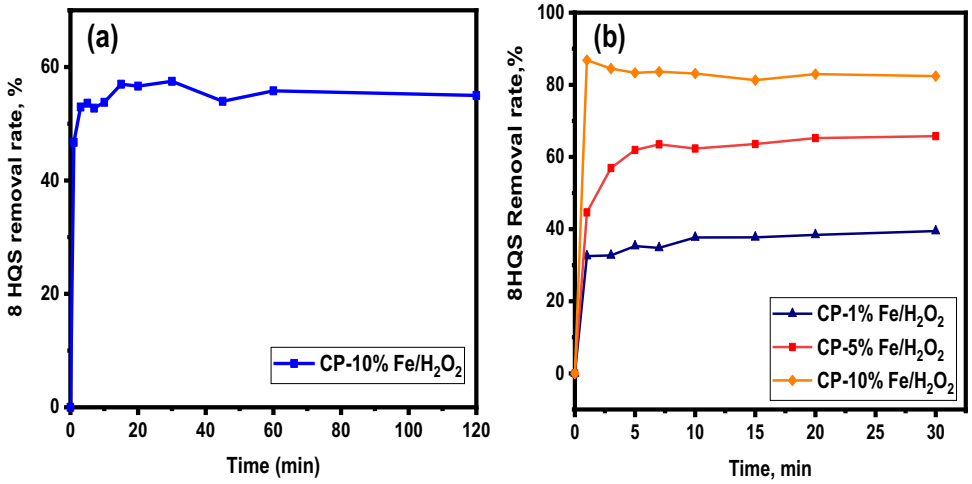

Fig. 5 **a** Effect of time on 8-HQS oxidation. $T = 30$ °C; pH = 11; [CP-10% Fe = 10 mg; H_2O_2/8-HQS = 27.5; [8-HQS] = 0.2 mM; $V_{8\text{-HQS}} = 100$ ml. **b** Effect of iron content on 8-HQS oxidation. $T = 30$ °C; [catalyst] = 15 mg; H_2O_2/8-HQS = 27.5; pH = 11; [8-HQS] = 0.2 mM; $V_{8\text{-HQS}} = 100$ ml

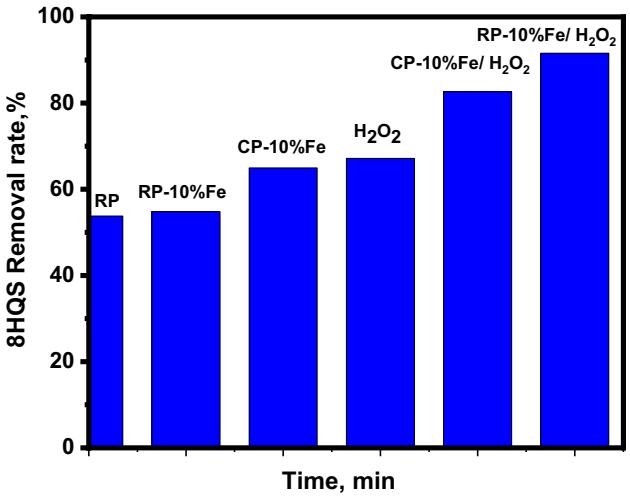

Fig. 6 Comparison of 8-HQS removal by different processes. $T = 30$ °C, [Catalyst] = 15 mg, pH = 11; H_2O_2/8-HQS = 27.5 mol/mol; [8-HQS] = 0.2 mM; $V_{8\text{-HQS}} = 100$ ml, reaction time = 60 min)

the heterogeneous catalytic oxidation of 8-HQS by iron-coated perlite, six experimental trials were carried out, as illustrated in Fig. 6.

For comparative purposes, raw perlite and the as-prepared catalysts were tested separately to demonstrate the Fenton catalytic oxidation process (Fig. 6). When the aqueous solution contaminated with 8-HQS is treated with CP-10% Fe, the removal rate by adsorption is the most relevant compared to that using RP and RP-10%Fe. In fact, upon heating to the calcination temperature, the pore size of CP increases resulting in high porosity along with strong adsorbability. With H_2O_2 only, the degradation rate of 8-HQS is estimated as 67.17%. The highest degradation efficiency of 8-HQS, assessed as 91.56%, is reached using RP-10%Fe coupled with H_2O_2 which proves its high catalytic activity over CP-10%Fe/H_2O_2. This behaviour is expected since, as shown earlier, RP-10%Fe is more loaded with iron ions than CP-10% Fe.

Effect of operating conditions on Fenton catalytic oxidation of 8-HQS

RP-10%Fe and CP-10% Fe exhibit high catalytic activity in the presence of H_2O_2 towards 8-HQS degradation. Various operating parameters (initial pH, catalyst type and load, oxidation ratio, temperature and the initial concentration of 8-HQS) that highly affect this phenomenon have been investigated for achieving the best removal efficiency at the lowest economic costs.

Effect of initial pH on 8-HQS degradation

The initial solution pH is an important control parameter for maintaining the effectiveness of the heterogeneous catalytic oxidation process. Overall, a good heterogeneous catalyst has to operate in a wide pH range. The removal rate of 8-HQS using RP-10% Fe and CP-10% Fe with H_2O_2 under different pH conditions is depicted in Fig. 7.

At pH values ranging from 4 to 9, low degradation efficiencies are recorded using CP-10%Fe (Fig. 7b). They did not exceed 11.34% given that ferrous complexes which react slowly with H_2O_2 are formed ($[Fe(OH)_2]^+$ ($4 < pH < 7$), $Fe(OH)_3$ (pH = 8)) thus reducing the effectiveness of the heterogeneous Fenton reaction. This phenomenon can decrease the efficiency of a Fenton system, as less Fe^{3+} and Fe^{2+} are present to react with H_2O_2 to generate radicals, and afterward, the regeneration of Fe^{2+} becomes the rate-limiting process step (Babuponnusami and Muthukumar 2014, Trabelsi 2011). The removal efficiency of both types of catalysts increases as the pH rises from 9 to 11, reaches the maximum at pH 11 then decreases sharply at pH 12. Within 30 min, the highest removal rates of 8-HQS reached at pH 11 in the presence of

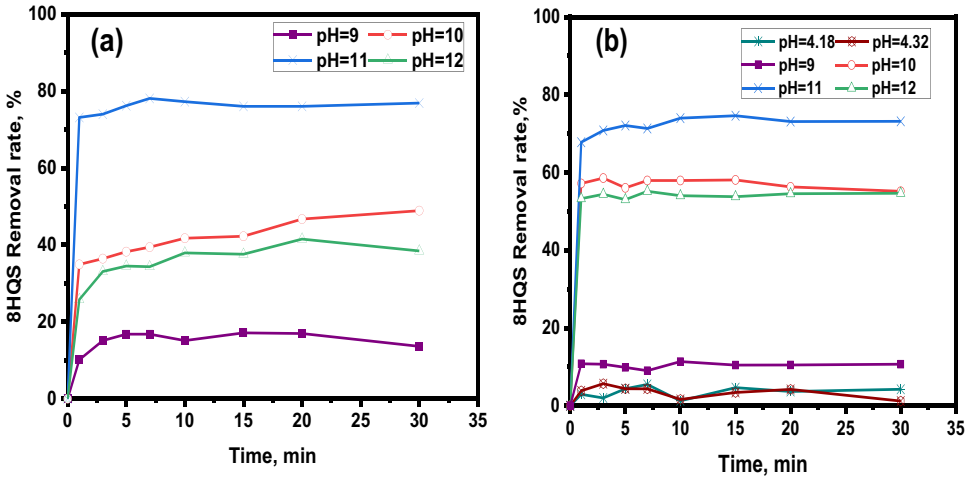

Fig. 7 **a** Effect of pH on 8-HQS oxidation using RP-10% Fe. $T = 30$ °C, [Catalyst] = 15 mg, H_2O_2/8-HQS = 27.5 mol/mol; [8-HQS] = 0.2 mM; $V_{8\text{-HQS}} = 100$ ml. **b** Effect of pH on 8-HQS oxidation using CP-10% Fe. $T = 30$ °C, [catalyst] = 25 mg, H_2O_2/8-HQS = 10 mol/mol; [8-HQS] = 0.2 mM; $V_{8\text{-HQS}} = 100$ ml)

RP-10% Fe and CP-10% are 77% and 73.18%, respectively. Considering the type of water matrix, it is worth to note that in the presence of both bicarbonate (HCO_3^-) and chloride (Cl^-) species, an optimum pH is required to reach the maximum of $^{\bullet}OH$ production, and this optimum pH value is recorded to shift toward a higher one as the molar ratio of Cl^-/HCO_3^- increases (Liao et al. 2001). Thus, it is highly suggested that a pH value of 11 is required to achieve a better process performance in the presence of both chloride and bicarbonate species. Interestingly, the degradation reaction can occur at alkaline conditions (pH > 9), indicating that the as-prepared catalysts can overcome the restricted pH range generally adopted in homogeneous Fenton oxidation systems (pH 2–4). Such behaviour could be related to the specific characteristics of catalyst, where iron cations are under the influence of a strong electrostatic field in the raw or calcined perlite structure that can prevent or postpone the formation of iron hydroxides as pH increases (pH 9–11) (Mirzaei et al. 2017). Moreover, the observed improvement can be assigned to the combination of both adsorption and catalytic oxidation processes. However, the decrease in 8-HQS removal efficiency at pH 12 may be due to the deactivation of the active site on the catalyst surface by the formation of iron complexes ($[Fe(OH)4]^-$) (pH ≥ 12) (Babuponnusami and Muthukumar 2014, Jiao et al. 2012, Trabelsi 2011) and/or lesser radical production. It is to highlight that the observed difference in the removal efficiencies between RP-10% Fe and CP-10% Fe at pH 10 and 12 can be attributed to the difference in catalyst load and molar oxidation ratio.

The above findings indicate that RP-10% Fe and CP-10% Fe are promising heterogeneous Fenton's catalysts at pH 11. Hence, it was decided to sustain pH 11 in the following experiments.

Effect of the catalyst load

The catalyst load is a highly important parameter affecting the Fenton catalytic oxidation process. Hence, its effect on the uptake of 8-HQS using RP-10% Fe and CP-10% Fe was studied and is shown in Fig. 8.

From this figure, it is clear that the catalyst dose affects positively the 8-HQS removal until 15 mg. Beyond this dose,

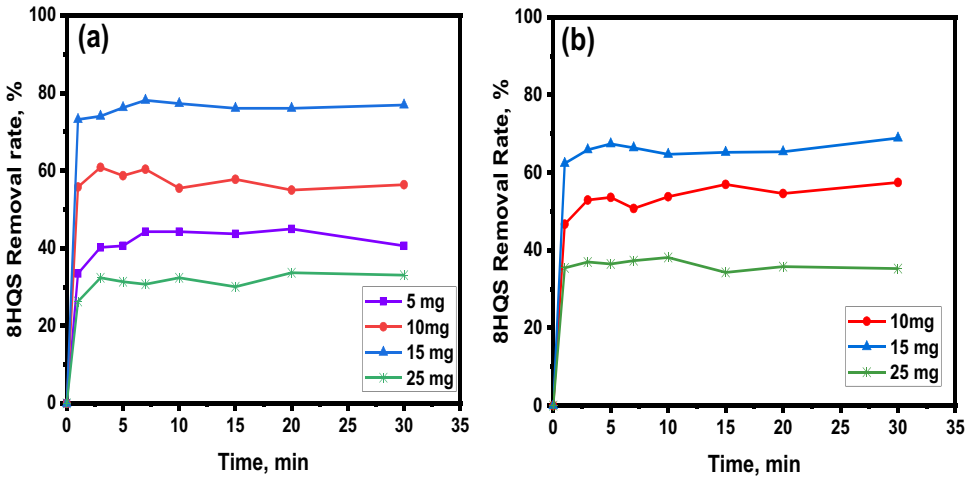

Fig. 8 **a** Effect of catalyst dose on 8-HQS oxidation using RR-10% Fe. $T = 30$ °C; H_2O_2/8-HQS = 27.5 mol/mol; pH = 11; [8-HQS] = 0.2 mM; $V_{8\text{-HQS}} = 100$ ml. **b** Effect of catalyst dose on 8-HQS oxidation using CP-10% Fe. $T = 30$ °C; H_2O_2/8-HQS = 10 mol/mol; pH = 11; [8-HQS] = 0.2 mM; $V_{8\text{-HQS}} = 100$ ml

further addition of the catalyst becomes inefficient and has a detrimental effect on the mineralization degree. This feature is characteristic of Fenton's reagent, and many authors have also found this kind of behaviour with heterogeneous systems (Buthiyappan et al. 2016, Herney-Ramirez et al. 2008, Herney-Ramirez and Madeira 2010, Jiang et al. 2017). The improvement in the removal rate can be attributed to the increased number of active sites able to generate a significant amount of hydroxyl radicals attacking the 8-HQS molecules. The removal rate may also be favoured by the adsorption owing to the high availability of the contact surface on the catalyst. However, at higher doses (25 mg), the reduction of the degradation rate might be probably due to the formation of iron complexes (iron and organics) (Herney-Ramirez et al. 2008, Herney-Ramírez and Madeira 2010) and/or the aggregation of catalyst particles, resulting in lower active surface area. The scavenging of different hydroxyl radicals by the Fe (R.1–3) and the water matrix species (chlorides, organic and inorganic carbon (carbonate and bicarbonate)) (R.4–6) (Mirzaei et al. 2017) may also explain this phenomenon, while many undesirable interactions between iron ions and other radicals (R.7) (Herney-Ramírez and Madeira 2010) could also be reported. Besides, it is worth noting that removal rates using RP-10% Fe are more significant than those reached using CP-10% Fe because more iron ions were incorporated on the raw perlite surface and a higher oxidation ratio was used; therefore, more radical production is expected. Whatever the nature of the used catalyst, a catalyst dose of 15 mg is highly recommended:

$$Fe^{2+} + {}^{\bullet}OH \rightarrow Fe^{3+} + OH^{-} \quad (1)$$

$$Fe^{2+} + HO_2^{\bullet} \rightarrow Fe^{3+} + HO_2^{-} \quad (2)$$

$$Fe^{3+} + HO_2^{\bullet} \rightarrow Fe^{2+} + O_2 + H^{+} \quad (3)$$

$$HCO_3^{-} + {}^{\bullet}OH \rightarrow H_2O + CO_3^{\bullet -} \quad (4)$$

$$CO_3^{2-} + {}^{\bullet}OH \rightarrow OH^{-} + CO_3^{\bullet -} \quad (5)$$

$$Cl^{-} + {}^{\bullet}OH \leftrightarrow ClHO^{\bullet -} \quad (6)$$

$$FeOH^{+} + {}^{\bullet}OH \rightarrow Fe^{3+} + 2OH^{-} \quad (7)$$

Effect of the molar oxidation ratio

The rate of catalysis activation and radical formation in the heterogeneous catalytic oxidation reaction is strongly dependent on the H_2O_2 concentration. So, the amount of H_2O_2 can be minimized by optimizing the molar oxidation ratio H_2O_2/8-HQS.

Whatever the used catalyst, the degradation rate of 8-HQS increases with increasing the molar oxidation ratio to a point at which further addition of H_2O_2 decreases slightly the removal rate (Fig. 9). In fact, the increase of H_2O_2 would increase the number of radicals suggesting the role of iron ions incorporated on the catalyst surface to make the Fenton reaction into action. Nevertheless, excessive H_2O_2 not only increases the operating costs but also enhances the scavenging effect of radicals by H_2O_2 Eq. (8), resulting in lower yield of degradation (Herney-Ramírez and Madeira 2010, Zhang et al. 2019). The optimal oxidation ratio for RP-10% Fe is 30 mol/mol (Fig. 9a), whereas it is only 27.5 for CP-10% Fe (Fig. 9b). This difference can be ascribed to the iron content incorporated on the catalyst surface and therefore to the yield of radical production as well as to the nature of the support:

$$H_2O_2 + {}^{\bullet}OH \rightarrow HO_2^{\bullet} + H_2O \quad (8)$$

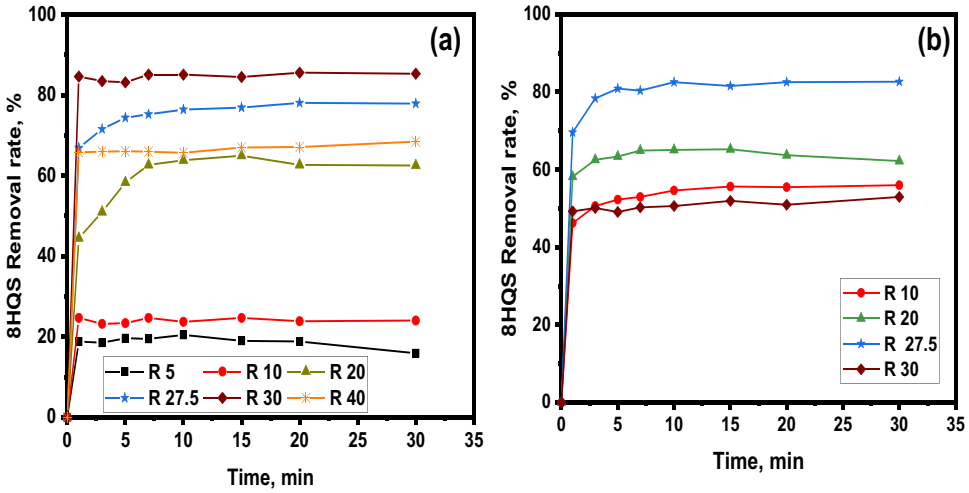

Fig. 9 **a** Effect of oxidation ratio on 8-HQS oxidation using RP-10% Fe. $T = 30$ °C; [catalyst] = 15 mg; pH = 11; [8-HQS] = 0.2 mM; $V_{8\text{-HQS}} = 100$ ml. **b** Effect of oxidation ratio on 8-HQS oxidation using CP-10% Fe. $T = 30$ °C; [catalyst] = 15 mg; pH = 11; [8-HQS] = 0.2 mM; $V_{8\text{-HQS}} = 100$ ml

Effect of temperature

Temperature is a critical parameter in Fenton processes since it influences the catalytic performance and stability of hydrogen peroxide. Moreover, the temperature may affect both the adsorption and oxidation processes. Hence, further studies were carried out to evaluate the optimal temperature that keeps effective the heterogeneous catalytic oxidation of 8-HQS.

According to Fig. 10, it is clear that the removal process depends strongly on the temperature. The highest removal rates assessed as 88.62% and 77.64% are reached within 30 min using RP-10%Fe and CP-10%Fe at 80 °C (Fig. 10a) and 30 °C (Fig. 10b), respectively. The difference in the optimal temperature can be ascribed to the nature, structure and characteristics of the used precursor (raw or calcined perlite). It is worth to note that temperature may enhance the adsorption by lowering the viscosity of the solution and breaking the interface layer around the catalyst particles. Moreover, with rising temperature, the rate of H_2O_2 decomposition by Fenton reaction increases resulting in more production of hydroxyl radicals (Carbajo et al. 2021; Wang 2008). The high catalytic activity and fast oxidation

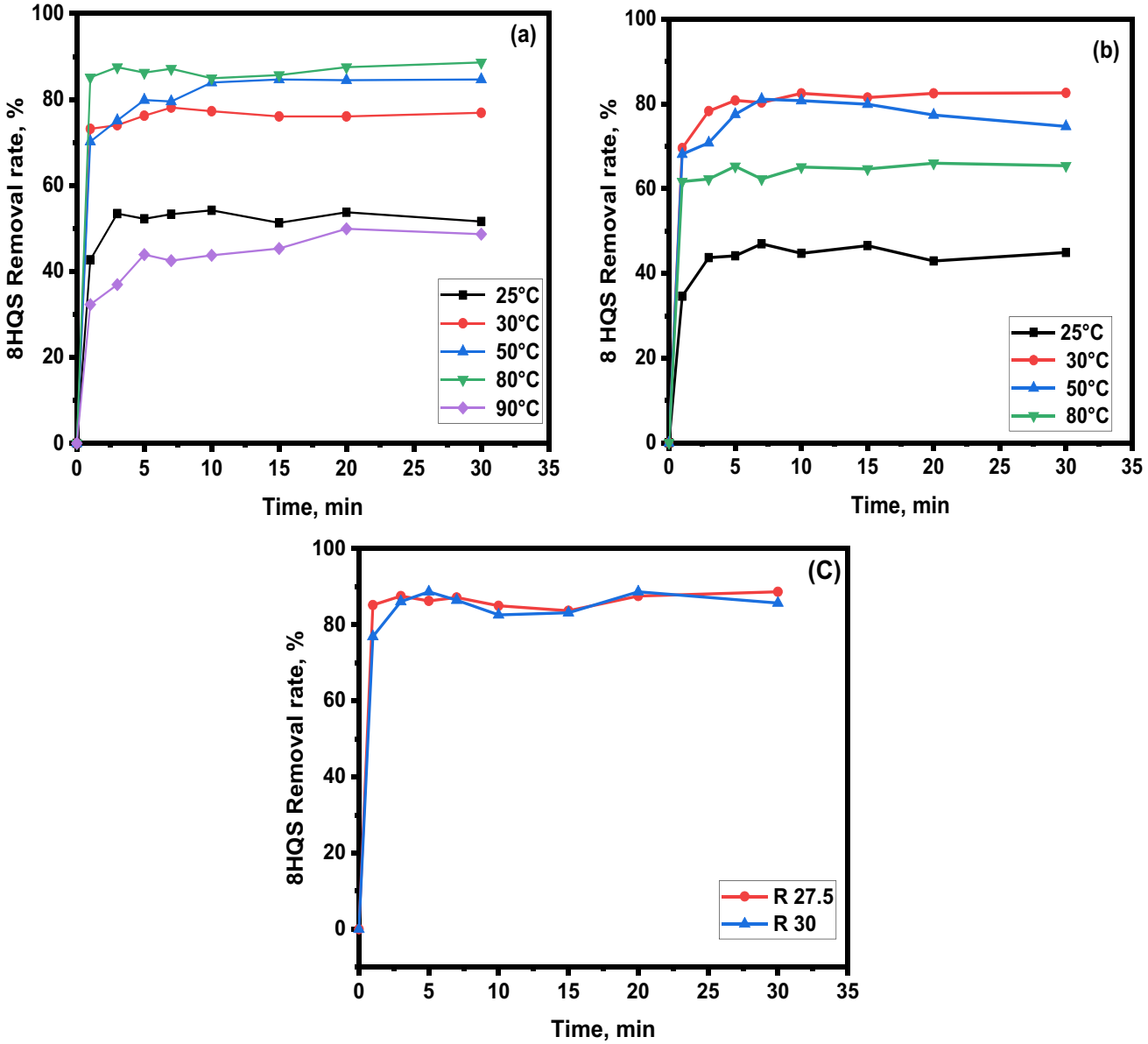

Fig. 10 **a** Effect of temperature on 8-HQS oxidation using RP-10% Fe. [Catalyst] = 15 mg; pH = 11; H_2O_2/8-HQS = 27.5 mol/mol; [8-HQS] = 0.2 mM, $V_{8\text{-HQS}}$ = 100 ml. **b** Effect of temperature on 8-HQS oxidation using CP-10%Fe. [Catalyst] = 15 mg; pH = 11; H_2O_2/8-HQS = 27.5 mol/mol; [8-HQS] = 0.2 mM, $V_{8\text{-HQS}}$ = 100 ml. **c** Effect of temperature on molar oxidation ratio using RP-10% Fe. *T* = 80 °C; [RP-10% Fe] = 15 mg; pH = 11; [8-HQS] = 0.2 mM, $V_{8\text{-HQS}}$ = 100 ml

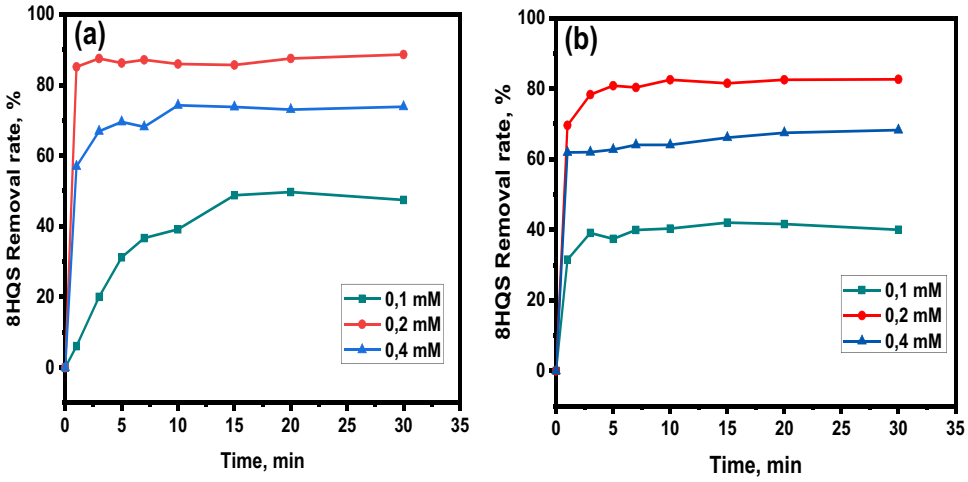

Fig. 11 **a** Effect of initial concentration on 8-HQS oxidation using RP-10% Fe. $T = 80$ °C; [catalyst] = 15 mg; pH = 11; H_2O_2/8-HQS = 27.5 mol/mol; $V_{8\text{-HQS}} = 100$ ml. **b** Effect of initial concentration on 8-HQS oxidation using CP-10% Fe. $T = 30$ °C; [catalyst] = 15 mg; pH = 11; H_2O_2/8-HQS = 27.5 mol/mol; $V_{8\text{-HQS}} = 100$ ml

kinetics of the RP-10%Fe, as compared to CP-10%Fe, can be assigned to the effective incorporation of higher iron content and the later formation of more active sites on its surface. However, increasing the temperature above these optimal values did not improve the kinetics of pollutant degradation, which can be ascribed to the desorption of molecules as a function of time.

To assess further the effect of the optimal temperature found in the case of RP-10%Fe ($T = 80$ °C) on the oxidation ratio, two runs were carried out at 27.5 and 30 mol/mol (Fig. 10c). The two molar oxidation ratios show quite similar behaviour, as there was no notable difference between them at 80 °C. For economic considerations, the molar oxidation ratio is assumed to be 27.5 mol/mol for both catalysts.

Effect of initial concentration of 8-HQS

The effect of the initial concentration on 8-HQS removal was investigated for values ranging from 0.1 to 0.4 mM.

According to Fig. 11, an enhancement in the 8-HQS removal rate occurs when the concentration increases from 0.1 to 0.2 mM due to the sufficient active sites on the catalyst surface able to generate more radicals at a faster rate for the mineralization process. Considering very short lifetime of hydroxyl radicals, increasing the initial concentration of 8-HQS will significantly enhance the collision between organic contaminants and ·OH, leading to an improvement in the degradation efficiency (Michael et al. 2010). At 0.2 mM, the maximum removal rates are 88.62% and 82.64% using RP-10% Fe and CP-10%, respectively. Beyond 0.2 mM, a significant decrease in the degradation efficiency is recorded. The same self-inhibiting effect of the 8-HQS initial concentration on the degradation efficiency was observed by several authors (Herney-Ramirez and Madeira 2010, Mirzaei et al. 2017, Shavisi et al. 2014). The decrease observed at 0.4 mM can be attributed to the competitive consumption of hydroxyl radicals by the increasing amount of 8-HQS molecules. On the other hand, as the initial concentration of the pollutant increases, more molecules of solute can be adsorbed on the surface of the catalyst, resulting in lower generation of ·OH radicals since the active sites are already occupied by 8-HQS molecules (Mirzaei et al. 2017; Zhang et al. 2009). These phenomena suggest that in the Fenton processes, the concentration of the optimal reagents (H_2O_2 and iron content) has to be assessed based on the initial concentration of organic contaminants to ensure their effective removal. Since

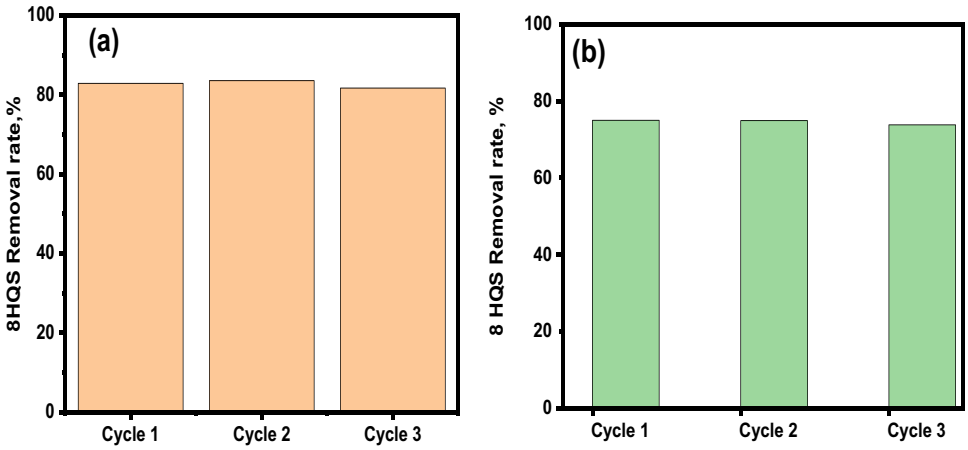

Fig. 12 **a** The recycled property of RP-10% Fe during 8-HQS oxidation. $T = 80$ °C; [Catalyst] = 15 mg; pH = 11; H_2O_2/8-HQS = 27.5 mol/mol; [8-HQS] = 0.2 mM; Reaction time = 1 h. **b** The recycled property of CP-10%Fe during 8-HQS oxidation. $T = 30$ °C; [Catalyst] = 15 mg; pH = 11; H_2O_2/8-HQS = 27.5 mol/mol; [8-HQS] = 0.2 mM; Reaction time = 1 h

Table 1 Concentration of iron ions leached in the solution after 8-HQS oxidation using (a) RP-10%Fe. $T = 80$ °C; [Catalyst] = 15 mg; pH = 11; H_2O_2/8-HQS = 27.5 mol/mol; [8-HQS] = 0.2 mM; reaction time = 1 h. (b) CP-10%Fe. $T = 30$ °C; [Catalyst] = 15 mg; pH = 11; H_2O_2/8-HQS = 27.5 mol/mol; [8-HQS] = 0.2 mM; reaction time = 1 h

	RP-10%Fe			CP-10%Fe		
Cycle	1	2	3	1	2	3
Iron loss (mg/L)	0.0274	0.0496	0.0513	0.0431	0.0429	0.0427

the concentration 0.2 mM always remains within the standard for industrial discharges of persistent pollutants, we will adopt it in our particular case at hand for the remaining experiments.

Reusability of catalyst

The stability and reusability of the as-prepared catalysts were assessed through a series of cycle experiments. The catalysts were reused three times for the degradation of 0.2 mM of 8-HQS solutions at the optimum conditions. Between each trial, the catalyst was filtered out and washed many times with distilled water before being dried at 60 °C overnight.

As seen in Fig. 12, the removal efficiency of 8-HQS using RP-10% Fe and CP-10%Fe is decreased by 1.2% and 1.5%, respectively, after three consecutive reaction runs, indicating that they are highly efficient and stable heterogeneous Fenton catalysts. Iron leaching is the main limitation of a heterogeneous catalyst that must be investigated. To assess its effect, concentrations of iron ions were detected in the solution after each cycle (Table 1). The obtained results show that the concentration of iron that has been leached out after 8-HQS oxidation is extremely low (< 0.1 mg/L) and respects the legal limit of 2 mg/L imposed by the directives of the European Union(Wang et al. 2015; Yao et al. 2017). Consequently, the synthesized catalysts have good stability against iron ion leaching, and they are easily recoverable for further reuse.

Performance comparison

The nature of the used catalyst affects strongly the heterogeneous catalytic oxidation process. So, the effect of two types of catalysts on 8-HQS degradation was evaluated. The first catalyst to be tested is a copper-based lamellar double hydroxide (Ni–Cu–Al–CO_3 LDH) that was developed in our laboratory research, and its results in terms of characterization and catalytic performance were reported in Hamdi et al. (2020). The second catalyst is an Al–Fe pillared clay (PILC-AlFe10%C with molar ratio Fe/(Al + Fe) = 10%) prepared according to the conventional method following the protocol reported by Sassi et al. (2017). The result of its characterization and catalytic performance will be reported in another paper.

According to the histogram presented in Fig. 13, RP-10%Fe and CP-10%Fe (at pH 11) are by far more efficient than LDH (at pH 4.5 and pH 11) and PILC-AlFe10%C (at pH 4) with respect to the degradation of 8-HQS. Accordingly, the as-synthesized catalysts show an undeniable advantage over these two catalysts. The reasons behind this would be attributed to the porous structure of perlite as well as the successful immobilization of iron on its surface.

Conclusion

Herein, efforts are conducted to set up the most efficient and cost-effective heterogeneous Fenton catalysts based on iron-coated perlite. The loading of perlite with iron oxide was performed by a direct and simple impregnation method. It seems that the porous

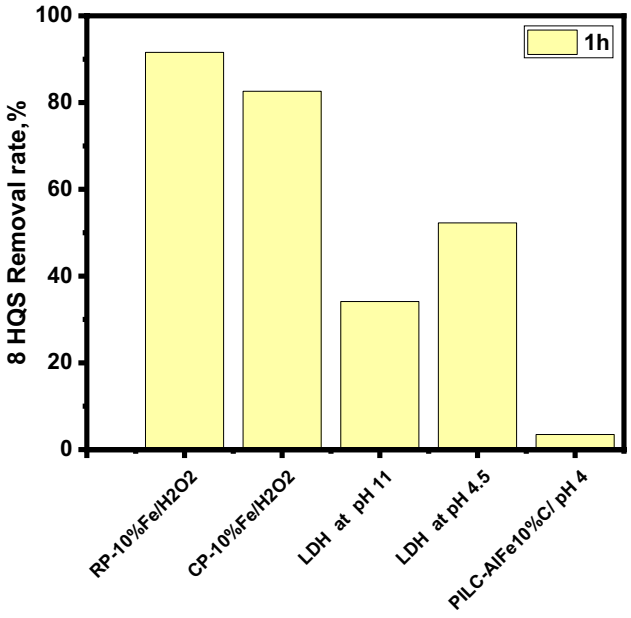

Fig. 13 Performance comparison between RP-10%Fe ($T = 80$ °C; [Catalyst] = 15 mg; pH = 11; H_2O_2/8-HQS = 27.5 mol/mol; [8-HQS] = 0.2 mM; $V_{8\text{-HQS}} = 100$ ml); CP-10%Fe ($T = 30$ °C; [Catalyst] = 15 mg; pH = 11; H_2O_2/8-HQS = 27.5 mol/mol; [8-HQS] = 0.2 mM; $V_{8\text{-HQS}} = 100$ ml); Ni–Cu–Al–CO_3 LDH ($T = 30$ °C; [Catalyst] = 15 mg; pH = 4.5 and 11; H_2O_2/8-HQS = 27.5 mol/mol; [8-HQS] = 0.2 mM; $V_{8\text{-HQS}} = 100$ ml) and PILC-AlFe10%C ($T = 30$ °C; [Catalyst] = 15 mg; pH = 4; H_2O_2/8-HQS = 27.5 mol/mol; [8-HQS] = 0.2 mM; $V_{8\text{-HQS}} = 100$ ml) during 8-HQS oxidation

structure of perlite helps the immobilization of iron species on its surface. The catalytic performances of the as-synthesized catalysts are significant in terms of 8-HQS degradation considering their large surface area and highly active surface sites. They function simultaneously as adsorbents and heterogeneous catalysts, causing the extremely rapid oxidation of the pollutant. On the other hand, the fabricated catalysts can operate in a wide pH range proving their effectiveness with respect to the heterogeneous catalytic oxidation process. The efficiency of iron-coated perlite samples is depending on the iron content on the perlite surface; the higher the iron ratio, the greater the oxidation of 8-HQS. The catalyst samples can be easily recovered and recycled several times, showing another advantage over the homogenous Fenton process.

Acknowledgements The authors acknowledge Professor Hassen Abdallah from the Energy Research and Technology Center (CRTEn, Hammam-Lif, Tunisia) for providing the digital processing units used to perform the microscopic image observation.

Author contribution All the authors contributed to the experimental study performed in the Laboratory of Wind Energy Control and Waste Energy Management (LMEEVED) (CRTEn). Material preparation, data collection and analysis were performed by BOUMNIJEL Ibtissem, HACHEM Houda, HAMDI Najwa, BEN AMOR Hedi and MIHOUBI Daoued. The first draft of the manuscript was written by BOUMNIJEL Ibtissem, and all the authors commented on previous versions of the manuscript. All the authors read and approved the final manuscript.

Funding The authors received financial support from the Ministry of Higher Education (TUNISIA).

Data availability Not applicable.

Declarations

Ethics approval This article does not contain any studies with human participants or animals performed by any of the authors.

Consent to participate All authors are aware of and accept responsibility for the manuscript.

Consent for publication No part of the manuscript contents has been published or has been accepted for publication elsewhere.

Conflict of interest The authors declare no competing interests.

References

Ahmed IM, Attia LA, Attallah MF (2020) Modification of perlite to prepare low cost zeolite as adsorbent material for removal of 144Ce and 152+154Eu from aqueous solution. Radiochim Acta 108:727–735

Babuponnusami A, Muthukumar K (2014) A review on Fenton and improvements to the Fenton process for wastewater treatment. J Environ Chem Eng 2:557–572

Bagdassarov N, Ritter, Yanev Y (1999) Kinetics of perlites degassing: TG and DSC analysis. Glass Sci Technol-Frankfurt am Main- 72:277–290

Baloyi J, Ntho T, Moma J (2018) Synthesis and application of pillared clay heterogeneous catalysts for wastewater treatment: a review. RSC Adv 8:5197–5211

Bautista P, Mohedano AF, Casas JA, Zazo JA, Rodriguez JJ (2008) An overview of the application of Fenton oxidation to industrial wastewaters treatment. J Chem Technol Biotechnol 83:1323–1338

Boddu VM, Hay KJ, Ghosh TK, Viswanath DS (2009) Method for surface treating perlite sorbents for improved adsorbing of vapor phase metals and metal compounds at elevated temperatures. US7524794B2

Brindha K, Amutha P, Krishnakumar B, do Nascimento Sobral AJF (2019) BiCl3-modified perlite as an effective catalyst for selective organic transformations: a green protocol. Res Chem Intermed 45:4367–4381

Briton BGH, Duclaux L, Richardson Y, Yao KB, Reinert L, Soneda Y (2019) Effectiveness of the dispersion of iron nanoparticles within micropores and mesopores of activated carbon for Rhodamine B removal in wastewater by the heterogeneous Fenton process. Appl Water Sci 9:166. https://doi.org/10.1007/s13201-019-1047-0

Buthiyappan A, Abdul Aziz AR, Wan Daud WMA (2016) Recent advances and prospects of catalytic advanced oxidation process in treating textile effluents. Rev Chem Eng 32:1–47

Carbajo J, Silveira JE, Pliego G, Zazo JA, Casas JA (2021) Increasing Photo-Fenton process Efficiency: the effect of high temperatures. Sep Purif Technol 271:118876. https://doi.org/10.1016/j.seppur.2021.118876

Dapaah MF, Niu Q, Yu Y-Y, You T, Liu B, Cheng L (2022) Efficient persistent organic pollutant removal in water using MIL-metal–organic framework driven Fenton-like reactions: a critical review. Chem Eng J 431:134182

Deng J, Dong H, Zhang C, Jiang Z, Cheng Y, Hou K, Zhang L, Fan C (2018) Nanoscale zero-valent iron/biochar composite as an activator for Fenton-like removal of sulfamethazine. Sep Purif Technol 202:130–137

Du C, Zhang Y, Zhang Z, Zhou L, Yu G, Wen X, Chi T, Wang G, Su Y, Deng F (2022) Fe-based metal organic frameworks (Fe-MOFs) for organic pollutants removal via photo-Fenton: a review. Chem Eng J 431:133932

Esmaielpour M, Akhlaghinia B, Jahanshahi R (2017) Green and efficient synthesis of aryl/alkylbis(indolyl)methanes using expanded perlite-PPA as a heterogeneous solid acid catalyst in aqueous media. J Chem Sci 129:313–328

Fontecha-Cámara MA, Álvarez-Merino MA, Carrasco-Marín F, López-Ramón MV, Moreno-Castilla C (2011) Heterogeneous and homogeneous Fenton processes using activated carbon for the removal of the herbicide amitrole from water. Appl Catal B 101:425–430

Grčić I, Obradović M, Vujević D, Koprivanac N (2010) Sono-Fenton oxidation of formic acid/formate ions in an aqueous solution: from an experimental design to the mechanistic modeling. Chem Eng J 164:196–207

Hamdi N, Proietto F, Ben Amor H, Galia A, Inguanta R, Ammar S, Gadri A, Scialdone O (2020) Effective removal and mineralization of 8-hydroxyquinoline-5-sulfonic acid through a pressurized electro-Fenton-like process with Ni−Cu−Al layered double hydroxide. ChemElectroChem 7:2457–2465

Hartmann M, Kullmann S, Keller H (2010) Wastewater treatment with heterogeneous Fenton-type catalysts based on porous materials. J Mater Chem 20(41):9002. https://doi.org/10.1039/c0jm00577k

Herney-Ramirez J, Lampinen M, Vicente MA, Costa CA, Madeira LM (2008) Experimental design to optimize the oxidation of Orange II dye solution using a clay-based Fenton-like catalyst. Ind Eng Chem Res 47:284–294

Herney-Ramírez J, Madeira LM (2010): Use of Pillared clay-based catalysts for wastewater treatment through Fenton-like processes. Pillared Clays and Related Catalysts pp 129–165. https://doi.org/10.1007/978-1-4419-6670-4_6

Jahanshahi R, Akhlaghinia B (2015) Expanded perlite: an inexpensive natural efficient heterogeneous catalyst for the green and highly accelerated solvent-free synthesis of 5-substituted-1H-tetrazoles using [bmim]N3 and nitriles. RSC Adv 5:104087–104094

Jiang L, Wang J, Wu X, Zhang G (2017) A stable Fe2O3/expanded perlite composite catalyst for degradation of rhodamine B in heterogeneous photo-Fenton system. Water Air Soil Pollut 228:12 . https://doi.org/10.1007/s11270-017-3646-4

Jiao C, Ji B, Fang D (2012) Preparation and properties of lauric acid–stearic acid/expanded perlite composite as phase change materials for thermal energy storage. Mater Lett 67:352–354

Joseph J, Iftekhar S, Srivastava V, Fallah Z, Zare EN, Sillanpaa M (2021) Iron-based metal-organic framework: Synthesis, structure and current technologies for water reclamation with deep insight into framework integrity. Chemosphere 284:131171

Khudr MS, Ibrahim YME, Garforth A, Alfutimie A (2021) On copper removal from aquatic media using simultaneous and sequential iron-perlite composites. J Water Proc Eng 40:101842. https://doi.org/10.1016/j.jwpe.2020.101842

Kolvari E, Koukabi N, Hosseini MM, Khandani Z (2015) Perlite: an inexpensive natural support for heterogenization of HBF4. RSC Adv 5:36828–36836

Liao CH, Kang SF, Wu FA (2001) Hydroxyl radical scavenging role of chloride and bicarbonate ions in the H2O2/UV process. Chemosphere 44:1193–1200

Maryami M, Nasrollahzadeh M, Mehdipour E, Sajadi SM (2017) Green synthesis of the Pd/perlite nanocomposite using Euphorbia neriifolia L. leaf extract and evaluation of its catalytic activity. Sep Purif Technol 184:298–307

Michael I, Hapeshi E, Michael C, Fatta-Kassinos D (2010) Solar Fenton and solar TiO2 catalytic treatment of ofloxacin in secondary treated effluents: evaluation of operational and kinetic parameters. Water Res 44:5450–5462

Mirzaei A, Chen Z, Haghighat F, Yerushalmi L (2017) Removal of pharmaceuticals from water by homo/heterogonous Fenton-type processes - a review. Chemosphere 174:665–688

Navalon S, Alvaro M, Garcia H (2010) Heterogeneous Fenton catalysts based on clays, silicas and zeolites. Appl Catal B 99:1–26

Navalon S, Dhakshinamoorthy A, Alvaro M, Garcia H (2011) Heterogeneous fenton catalysts based on activated carbon and related materials. Chemsuschem 4:1712–1730

Papa E, Medri V, Natali Murri A, Laghi L, De Aloysio G, Bandini S, Landi E (2018) Characterization of alkali bonded expanded perlite. Constr Build Mater 191:1139–1147

Poza-Nogueiras V, Arellano M, Rosales E, Pazos M, Sanromán MA, González-Romero E (2018) Electroanalytical techniques applied to monitoring the electro-Fenton degradation of aromatic imidazolium-based ionic liquids. J Appl Electrochem 48:1331–1341

Puga A, Rosales E, Pazos M, Sanromán MA (2020) Prompt removal of antibiotic by adsorption/electro-Fenton degradation using an iron-doped perlite as heterogeneous catalyst. Process Saf Environ Prot 144:100–110

Ramirez JH, Maldonado-Hódar FJ, Pérez-Cadenas AF, Moreno-Castilla C, Costa CA, Madeira LM (2007) Azo-dye Orange II degradation by heterogeneous Fenton-like reaction using carbon-Fe catalysts. Appl Catal B 75:312–323

Roulia M, Chassapis K, Kapoutsis JA, Kamitsos EI, Savvidis T (2006) Influence of thermal treatment on the water release and the glassy structure of perlite. J Mater Sci 41:5870–5881

Sassi H, Lafaye G, Ben Amor H, Gannouni A, Jeday MR, Barbier J (2017) Wastewater treatment by catalytic wet air oxidation process over Al-Fe pillared clays synthesized using microwave irradiation. Front Environ Sci Eng 12:2. https://doi.org/10.1007/s11783-017-0971-1

Saufi H, El Alouani M, Alehyen S, El Achouri M, Aride J, Taibi Mh (2020) Photocatalytic degradation of methylene blue from aqueous medium onto perlite-based geopolymer. Int J Chem Eng 2020:1–7

Shavisi Y, Sharifnia S, Hosseini SN, Khadivi MA (2014) Application of TiO2/perlite photocatalysis for degradation of ammonia in wastewater. J Ind Eng Chem 20:278–283

Soufi A, Hajjaoui H, Elmoubarki R, Abdennouri M, Qourzal S, Barka N (2021) Spinel ferrites nanoparticles: synthesis methods and application in heterogeneous Fenton oxidation of organic pollutants – a review. Appl Surf Sci Adv 6:100145

Tekin H, Bilkay O, Ataberk SS, Balta TH, Ceribasi IH, Sanin FD, Dilek FB, Yetis U (2006) Use of Fenton oxidation to improve the biodegradability of a pharmaceutical wastewater. J Hazard Mater 136:258–265

Trabelsi S (2011) Etudes de traitement des lixiviats des déchets urbains par les procédés d'oxydation avancée photochimiques et électrochimiques: application aux lixiviats de la décharge tunisienne "Jebel Chakir". Sciences de la Terre, Université Paris-Est Français. NNT: 2011PEST1122

Wang F-X, Wang C-C, Du X, Li Y, Wang F, Wang P (2022) Efficient removal of emerging organic contaminants via photo-Fenton process over micron-sized Fe-MOF sheet. Chem Eng J 429:132495. https://doi.org/10.1016/j.cej.2021.132495

Wang N, Zheng T, Zhang G, Wang P (2016) A review on Fenton-like processes for organic wastewater treatment. J Environ Chem Eng 4:762–787

Wang S (2008) A comparative study of Fenton and Fenton-like reaction kinetics in decolourisation of wastewater. Dyes Pigm 76:714–720

Wang Y, Sun Y, Li W, Tian W, Irini A (2015) High performance of nanoscaled Fe2O3 catalyzing UV-Fenton under neutral condition with a low stoichiometry of H2O2: Kinetic study and mechanism. Chem Eng J 267:1–8

Xu M, Wu C, Zhou Y (2020) Advancements in the Fenton process for wastewater treatment. Advanced Oxidation Processes, Applications, Trends, and Prospects 61. https://doi.org/10.5772/intechopen.90256

Yao H, Xie Y, Jing Y, Wang Y, Luo G (2017) Controllable preparation and catalytic performance of heterogeneous Fenton-like α-Fe2O3/crystalline glass microsphere catalysts. Ind Eng Chem Res 56:13751–13759

Zhang H, Fu H, Zhang D (2009) Degradation of C.I. Acid Orange 7 by ultrasound enhanced heterogeneous Fenton-like process. J Hazard Mater 172:654–660

Zhang MH, Dong H, Zhao L, Wang DX, Meng D (2019) A review on Fenton process for organic wastewater treatment based on optimization perspective. Sci Total Environ 670:110–121